

Signal buffering in random networks of spiking neurons: Microscopic versus macroscopic phenomena

Julien Mayor and Wulfram Gerstner*

Brain-Mind Institute and School of Computer and Communication Sciences, Ecole Polytechnique Fédérale de Lausanne (EPFL), CH-1015 Lausanne, Switzerland

(Received 11 February 2005; revised manuscript received 5 July 2005; published 3 November 2005)

In randomly connected networks of pulse-coupled elements a time-dependent input signal can be buffered over a short time. We studied the signal buffering properties in simulated networks as a function of the networks' state, characterized by both the Lyapunov exponent of the microscopic dynamics and the macroscopic activity derived from mean-field theory. If all network elements receive the same signal, signal buffering over delays comparable to the intrinsic time constant of the network elements can be explained by macroscopic properties and works best at the phase transition to chaos. However, if only 20% of the network units receive a common time-dependent signal, signal buffering properties improve and can no longer be attributed to the macroscopic dynamics.

DOI: [10.1103/PhysRevE.72.051906](https://doi.org/10.1103/PhysRevE.72.051906)

PACS number(s): 87.18.Sn, 82.40.Bj, 87.10.+e

I. INTRODUCTION

Neurons in the brain are connected with each other and send short electrical pulses (action potentials or spikes) along those connections. Despite the fact that there are correlations between the type of connections and the type of neurons [1], it is fair to say that neurons fall essentially into two classes, excitatory and inhibitory, and that the connectivity in a local population of several thousand cortical neurons is close to random. Networks with fixed random connectivity can, in principle, contain loops of varying size, which could sustain the flow of transient information signals over times that are long compared to the intrinsic time constants of the network elements, i.e., the neurons. In neuroscience and related fields, elementary considerations on information flow in random networks have inspired ideas as diverse as synfire chain activity [2], reverberations [3], liquid computing [4], echo state machines [5], or computing at the edge of chaos [6,7]. At the center of all these ideas is the concept that the network state must be characterized on a microscopic level. In other words, the identity of the active neurons is relevant so that an activity pattern where, say, neurons number 17, 43, 387, 557, and 621 are active together is different from a network state where a different subset of neurons is active. The differences between microscopic network states can be measured by the differences in the membrane potential of all N neurons. The evolution of these differences over time can be characterized by a Lyapunov exponent.

On the other hand, random networks have also been studied intensively by the physics community, in the context of diluted spin glasses [8], formal neural networks [9,10], or automata [11] and limiting cases have been identified for which exact solutions are known. In particular, in the limit of asymmetric networks with low connectivity, mean-field dynamics becomes exact [10]. More recently these approaches have been extended to the case of random networks of spik-

ing neurons in continuous time [12]. In a mean-field approach, the state of the network is fully characterized by a macroscopic activity variable, i.e., the fraction of neurons that are active per unit of time. Hence the identity of the active neurons is irrelevant.

In this paper, we will compare simulations of a random network of excitatory and inhibitory neurons with the mean-field solutions valid in the low-connectivity limit and evaluate the performance of such networks on a simple information buffering task that can be seen as a minimal and necessary requirement for more complex computational tasks [4,5] which a neural network might have to solve. More precisely, the task consists in reconstructing a time-dependent input $I(t')$ by reading out the activity of the network at a later time $t=t'+\Delta$. The readout will be performed in two conceptually different ways: a "microscopic" readout that combines the activity of all N neurons with N different weighting factors; and a "macroscopic" readout that gives the same weight to all neurons. While the microscopic readout is sensitive to the identity of the individual neurons, the macroscopic readout is only sensitive to the fraction of neurons that are active per unit of time.

We will see that performance in the information buffering task is best at the phase transition that is marked by a rapid increase in both the *macroscopic* activity variable and the Lyapunov exponent characterizing the *microscopic* network state indicating transition to chaos. Moreover, if the same time-dependent input $I(t)$ is shared by all neurons in the network, a macroscopic information readout based only on the fraction of active neurons is as good as a microscopic readout that is based on the output pulses of all N neurons. However, if the input is only given to a small group of neurons a detailed readout conveys more information than a macroscopic one. This indicates that the identity of active neurons plays a role, as predicted by theories postulating information flow along loops in the network connectivity. In contrast to those theories, we find that the maximum information buffering delay is in the range of the intrinsic time constant of the network elements (i.e., the membrane time constant of

*Electronic address: wulfram.gerstner@epfl.ch

the neurons) and that the amount of information buffered in our random network is rather limited.

II. MODEL

We consider a network of N leaky integrate-and-fire units (neurons) with fixed random connectivity. Eighty percent of the neurons are taken as excitatory and the remaining 20% inhibitory. Independent of the network size ($N=200, 400, 800$), each neuron i in our simulation receives input from $C_E=40$ excitatory and $C_I=10$ inhibitory units (presynaptic neurons), which are chosen at random amongst the $N-1$ other neurons in the network. The ensemble of neurons that are presynaptic to neuron i is denoted by M_i and the efficacy w_{ij} of a connection from a presynaptic neuron $j \in M_i$ to a postsynaptic neuron i is $w_{ij}=w_E$ if j is excitatory, and $w_{ij}=w_I$ if j is inhibitory.

Each neuron is described by a linear equation combined with a threshold. In the subthreshold regime the membrane potential follows the differential equation

$$\tau_m \dot{u}_i(t) = -u_i(t) + I_i^{\text{netw}} + I_i^{\text{ext}}(t), \quad (1)$$

where $\tau_m=20$ ms is the effective membrane time constant and I_i^{ext} is the external input. The recurrent input I_i^{netw} neuron i receives from the network is

$$I_i^{\text{netw}}(t) = \tau_m \sum_{j \in M_i} \omega_{ij} \sum_k \delta(t - t_j^k - D), \quad (2)$$

where t_j^k is the time neuron j fires its k th spike and $D=1$ ms is a short transmission delay. A spike from an excitatory (inhibitory) neuron $j \in M_i$ causes a jump in the membrane potential of neuron i of $w_E=0.6$ mV ($w_I=-3.6$ mV). If the membrane potential u_i reaches a threshold $\vartheta=10$ mV, a spike of neuron i is recorded and its membrane potential is reset to $u_i=0$. Integration restarts after an absolute refractory period of $\tau_{\text{rp}}=2$ ms.

The external input $I_i^{\text{ext}}=I_i^{\text{sg}}(t)+I_i^{\text{backg}}(t)$ can be separated into two components which we now discuss in turn

Test signal. We inject a time dependent test signal $I_i^{\text{sg}}(t)$ which is generated as follows: the total simulation time is broken into segments of duration $T_{\text{sg}}=10$ ms. During each segment of length T_{sg} the input is kept constant. At the transition to the next segment, a new value of $I_i^{\text{sg}}(t)$ is drawn from a uniform distribution over the interval $[-0.25, 0.25]$, i.e., the signal distribution has a standard deviation of $\sigma_{\text{sg}}=0.25/\sqrt{3}=0.144$. By construction the signal at time t provides no information about the signal at $t-T$ for $T>T_{\text{sg}}$. More precisely, the autocorrelation $A(s)$ of the signal has a triangular shape and is strictly zero for $|s|>T_{\text{sg}}$.

Background noise. The network of N neurons is considered as part of a larger brain structure. To mimic input from excitatory ‘‘background’’ neurons that are not modelled explicitly, we assume stochastic spike arrival described by a Poisson process of total rate ν_{exc} , i.e., the number of background spikes $n^{\text{backg}}(t;t+\Delta t)$ arriving in a time step Δt is Poisson distributed with mean $\nu_{\text{exc}}\Delta t$. For the sake of simplicity, we assume that the efficacy w_E of background spikes is identical to that of the recurrent connections within the

network. Thus the background input I^{backg} integrated over a time step Δt is $I^{\text{backg}}\Delta t = \tau_m w_E n^{\text{backg}}(t;t+\Delta t)$. For the theoretical analysis in Sec. III, we approximate the background input I^{backg} by a Gaussian white noise with mean $\langle I^{\text{backg}} \rangle = \mu^{\text{backg}} = \omega_E \nu_{\text{exc}} \tau_m$ and standard deviation $\sigma^{\text{backg}} = [(\langle (I^{\text{backg}} - \mu^{\text{backg}})^2 \rangle)^{1/2}] = \omega_E \sqrt{\nu_{\text{exc}} \tau_m}$, where ν_{exc} is the background spike arrival rate. This approximation is valid under the assumption that a neuron receives a large number of presynaptic contributions per unit time, each generating a change in the membrane potential that is relatively small compared to the firing threshold. To simplify notation we set $\gamma = C_I/C_E$ and $g = -\omega_I/\omega_E$. The values in our simulations are $\gamma=0.25$ and $g=6$.

III. CHARACTERIZING THE NETWORK STATE

The macroscopic variable describing the activity of the network is the population rate $\nu(t)$ defined by the fraction of neurons that are active in a time step divided by the duration of the time step. We will use a mean-field analysis of the random network in order to derive the population rate in a stationary state of asynchronous neuronal activity [12]. To do so, we approximate the triangular test signal I^{sg} that is used for the simulations by Gaussian white noise of zero mean and standard deviation σ_{sg} ; and the Poisson background noise used in the simulations by Gaussian white noise with mean μ^{backg} and standard deviation σ^{backg} . In the mean-field theory that is valid for low random connectivity in the limit of a large network ($N \rightarrow \infty$) [12], the stationary population rate approaches a constant value ν_0 that is identical to the mean firing rate of an arbitrarily chosen neuron in the network. The mean firing rate, and hence the population rate ν_0 , depend on the mean

$$\mu_0 = \omega_E \tau_m [\nu_{\text{exc}} + C_E \nu_0 (1 - g\gamma)]. \quad (3)$$

and variance

$$\sigma_0^2 = \omega_E^2 \tau_m^2 [\nu_{\text{exc}} + C_E \nu_0 (1 + g^2 \gamma)] + \sigma_{\text{sg}}^2 \quad (4)$$

of the total input $I^{\text{netw}} + I^{\text{ext}}$ via the equation

$$\frac{1}{\nu_0} = \tau_{\text{rp}} + 2\pi \int_{-\mu_0/\sigma_0}^{(\vartheta - \mu_0)/\sigma_0} du e^{u^2} \int_{-\infty}^u dv e^{-v^2}. \quad (5)$$

Combining Eqs. (3)–(5), we obtain a self-consistent solution of the population firing rate ν_0 as a function of the external Poisson drive ν_{exc} . We emphasize that by changing the background spike arrival rate ν_{exc} , we change both the mean drive μ_0 and the variance σ_0^2 . The inset of Fig. 1 shows the population rate ν_0 predicted by the mean-field theory as a function of the background spike arrival rate ν_{exc} . For small signal amplitudes ($\sigma_{\text{sg}} \rightarrow 0$), the population rate exhibits a first-order phase transition with coexistence of several solutions which disappears for larger signal amplitudes.

The main graph in Fig. 1 shows a simulation of a random network while stimulated with the test signal as explained in Sec. II. The population rate shows a marked increase near $\nu_{\text{exc}} \cong 420$ Hz (shown in Fig. 1) which is in the vicinity of the first-order phase transition predicted by the mean-field theory.

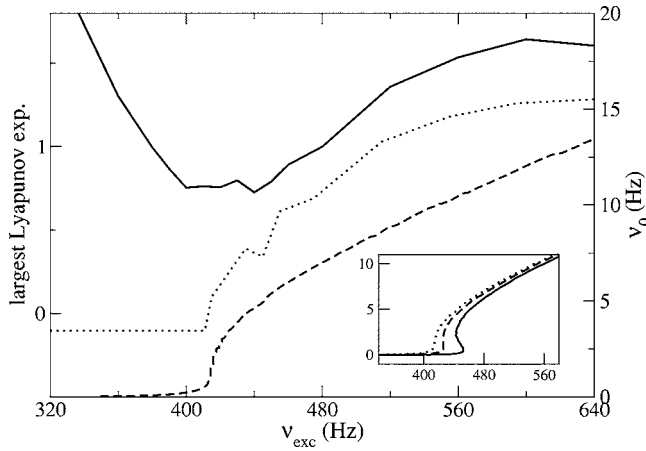


FIG. 1. Dashed line: Fixed points of the population activity ν_0 as a function of the Poisson background drive resulting from Eqs. (3)–(5). Note the sharp transition at $\nu_{\text{exc}}=420$ Hz. The network switches from an almost quiescent state to a state of sustained activity. Dotted line: largest Lyapunov exponent (see definition in text) as a function of the external drive ν_{exc} in a network of 800 neurons. For $\nu_{\text{exc}} < 420$ Hz the population rate ν_0 is low (“quiescent state”) and the largest Lyapunov exponent is negative. For a stronger drive, the exponent switches to a positive value, reflecting the chaotic behavior of the membrane potential trajectories. Solid line: Signal reconstruction error (arbitrary scale; for quantitative values see Fig. 2), as defined in text, for a delay of 20 ms in a network of 800 neurons. The error is minimal near the transition from the quiescent to a chaotic regime. Inset: Fixed points of the population rate [Eq. (5)] in absence of test signal (solid line), and with increasing signal variance. The system exhibit a first-order phase transition if the signal is weak.

By construction, a mean-field theory yields only a macroscopic description of the network activity. In order to get some insight into the microscopic network state, we considered the Lyapunov exponent of membrane potentials during simulations of the random network. The largest Lyapunov exponent is defined by $\lambda_p = \lim_{t \rightarrow \infty} \ln[\epsilon(t)/\epsilon(0)]$ where $\epsilon(t) = \sum_{i=1}^N [u_i(t) - u'_i(t)]^2$ is the difference between a reference trajectory of the N variables $u_1(t), \dots, u_N(t)$ and test trajectory $u'_1(t), \dots, u'_N(t)$ with slightly different initial conditions. Using standard numerical techniques [13], the largest Lyapunov exponent has been estimated from a large number of simulations of a test network and a reference network with identical connectivity. Both networks received identical input (same realization of the Poisson input and signal input) and the test trajectory was regularly reset close to the reference trajectory.

We found that the marked increase in the macroscopic variable ν_0 as a function ν_{exc} that has been predicted by the mean-field theory and confirmed in simulations (Fig. 1, dashed line) is accompanied by a transition of the largest Lyapunov exponent from negative to positive values (see dotted line in Fig. 1). This indicates that the microscopic dynamics becomes chaotic. Moreover, we confirmed that not only for background spike input but also for appropriately chosen constant input (i.e., $\mu^{\text{backg}} > 0$, $\sigma^{\text{backg}} = 0$), the fixed random connectivity is sufficient to generate irregular asyn-

chronous spiking activity [12] with a positive largest Lyapunov exponent (data not shown).

IV. INFORMATION BUFFERING

After having characterized the macroscopic and microscopic state of the network, we asked how performance in an information buffering task, inspired by concepts of liquid computing [4] and echo state machines [5], would depend on the network state. We considered a linear readout unit with dynamics

$$dy/dt = -[(y - \alpha_0)/\tau_s] + \sum_{i=1}^N \alpha_i \sum_k \delta(t - t_i^k), \quad (6)$$

where the sums run over all firing times t_i^k of all neurons in the network. $\tau_s = 5$ ms is a short synaptic time constant. We note that there are $N+1$ free parameters, a bias term α_0 plus one weighting factor α_i ($1 \leq i \leq N$) per neuron, i.e., different neurons are potentially treated differently (“microscopic readout”). These parameters are chosen so as to minimize the signal reconstruction error $E = \langle [y(t) - I^{\text{sg}}(t - \Delta)]^2 \rangle / \sigma_{\text{sg}}^2$. The performance depends on the delay Δ of information buffering which has to be compared with the membrane time constant ($\tau_m = 20$ ms) and the autocorrelation of the input $T_{\text{sg}} = 10$ ms. Parameters were optimized using a first simulation (learning set) lasting 100 s (100 000 time steps of simulation) and were kept fixed afterwards. The performance measurements reported in this paper are then evaluated on a second simulation of 100 s (test set). Simulation results were obtained using the simulation software NEST [15].

The same time-dependent signal $I^{\text{sg}}(t)$ was injected into all neurons in the network and the performance evaluated in terms of the signal reconstruction error. Overall the signal reconstruction error is relatively high. As expected, the signal reconstruction error increases if we increase the desired buffer duration from $\Delta = 10$ ms to $\Delta = 15$ ms or $\Delta = 20$ ms [Fig. 2(A)].

At the same time, the optimal background firing rate ν_{exc} to achieve minimal signal reconstruction error shifts towards lower values and is for $\Delta = 20$ ms very close to the transition between regular and chaotic microscopic dynamics as shown in Fig. 1. This result is consistent with the idea of computing at the edge of chaos in cellular automata [7] or threshold gates [6]. Also, similar to the results in discrete-time spin networks [14], the information buffering performance does not significantly depend on the number N of neurons in the network; cf. Fig. 2(B). Differences are within the statistical variations caused by overfitting on finite data samples.

V. MICROSCOPIC VS MACROSCOPIC PROPERTIES

Given that networks states have been classified successfully by macroscopic mean-field equations [12], we wondered whether the performance in the above information buffering task can be completely understood in terms of *macroscopic* quantities. To answer this question, we compared the performance using the previous readout unit y (i.e., a microscopic readout with $N+1$ free parameters, one per

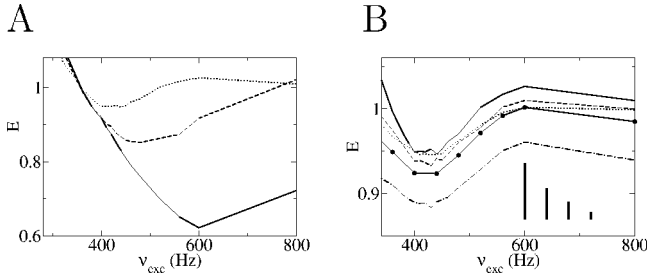


FIG. 2. (A) Signal reconstruction error E as a function of the background firing rate in a network of 800 neurons for three different information buffer delays: $\Delta=10$ ms (solid), $\Delta=15$ ms (dashed), $\Delta=20$ ms (dotted). For sufficiently long delays, optimal performance is located near the transition between the quiescent and the chaotic state; cf. Fig. 1. Deeper in the chaotic phase the error goes back to the chance level whereas in the almost quiescent regime we can see the effects of overfitting ($E > 1$), because the number of action potentials is insufficient to build an accurate model of the past events. (B) Comparison of the errors for different network sizes. Top three lines: Reconstruction error based on a *microscopic* readout in a network with $N=800$ neurons (solid line), $N=400$ neurons (dashed line), and $N=200$ neuron (dotted line) for a delay $\Delta=20$ ms. The fourth line from top (solid line with filled circles) shows the error based on a *macroscopic* readout of the network of $N=800$ neurons. The vertical shift of the error curves is not significant but due to overfitting because of limited amount of data. Vertical bars indicate the mean difference between errors on the data used for parameter optimization (training set) and that on an independent test set for $N=800$ (left bar), $N=400$ (second bar), $N=200$ (third bar) and macroscopic readout (right bar). A representative curve of errors on the *training set* for $N=800$ neurons is shown by the dot-dashed line (bottom). The location of minimal error is independent of the number of neurons or readout method and coincides with the phase transition indicated in Fig. 1.

neuron plus an offset) with that by a simplified readout \tilde{y} with two free parameters $\tilde{\alpha}$ and $\tilde{\beta}$ only,

$$d\tilde{y}/dt = -[(\tilde{y} - \tilde{\beta})/\tau_s] + \tilde{\alpha} \sum_{i=1}^N \sum_k \delta(t - t_i^k), \quad (7)$$

i.e., a readout that uses only the macroscopic population activity. Surprisingly, for a stimulation paradigm where all neurons receive the same time-dependent signal $I^{sg}(t)$ the macroscopic readout performs as well as the microscopic one. In other words, connectivity loops between *specific* subsets of neurons where signals could circulate for some time seem not to play a role in information buffering. This suggests that, for signals of sufficiently small amplitude, the information buffering capacity is directly related to the *macroscopic* linear response kernel κ of the network activity, that can, in principle, be calculated from the linearized mean-field equations of the population rate, i.e., $\Delta v(t) = \int \kappa(s) I^{sg}(t-s) ds$; cf. Ref. [12]. The time constant of the kernel, and hence information buffering delays, become large in the vicinity of a phase transition.

We hypothesized that signal transmission loops in our randomly connected network could manifest themselves more easily if only a small subset of neurons received the

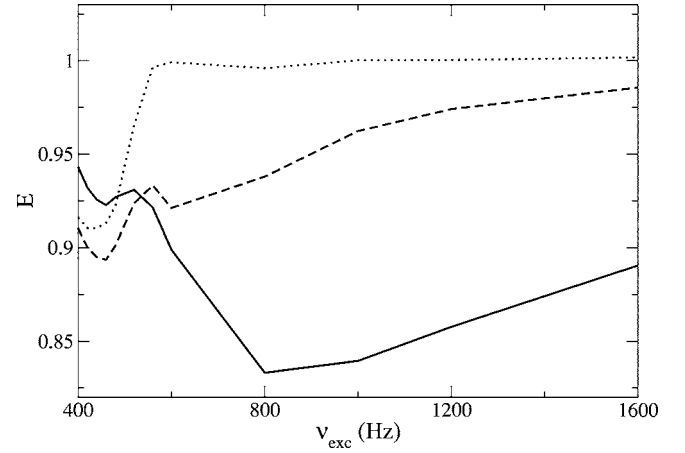


FIG. 3. The input is injected to 20% of the neurons only. A macroscopic readout assuming a single population (dotted line) performs well near the phase transition. However, deeper in the chaotic phase it is outperformed by the *microscopic* readout (solid line). A macroscopic readout based on a two-population assumption (dashed line) explains only part of the increased performance. The signal buffering delay for this figure is $\Delta=20$ ms.

input signal. We therefore selected 20% of neurons at random (group G_1) and injected an identical time-dependent signal $I_j^{sg}(t)$ into all neurons $j \in G_1$. The remaining 80% of neurons (group G_2) received no signal. In such a network consisting of two groups, signal buffering performance is indeed significantly better than in a single homogeneous group (Fig. 3). While the overall performance is never very good (the errors fall never below 0.8), the difference between a macroscopic and a microscopic readout is highly significant.

On a macroscopic scale, a network consisting of two groups G_1 and G_2 can be described by two macroscopic variables, i.e., the population activities in groups G_1 and G_2 . In order to evaluate the information contained in the macroscopic population rates, we used a linear readout unit y_2 with three free parameters β_0, β_1 , and β_2 , characterized by the differential equation $dy_2/dt = -[(y_2 - \beta_0)/\tau_s] + \beta_1 \sum_{i \in G_1} \sum_k \delta(t - t_i^k) + \beta_2 \sum_{i \in G_2} \sum_k \delta(t - t_i^k)$ and proceeded as before. As we can see from Fig. 3, a readout based on the macroscopic activity of the two groups performs significantly worse than the microscopic readout. This suggests, that for the case when only a small subset of units in a random network receive an input, signal transmission loops, and hence microscopic neuronal dynamics, indeed play a role in short-term information buffering. However, we emphasize that errors are consistently high indicating that the performance of a random network in a simple signal buffering task is not satisfying even if the required buffering time is only of the duration of one membrane time constant.

VI. DISCUSSION

A. Mean-field vs microscopic dynamics

Mean-field methods neglect correlations in the input. In random networks mean-field theory becomes asymptotically

correct only in the low-connectivity limit where the probability of closed loops tends to zero [10]. However, it is exactly these loops which could give the network the power to buffer information for times significantly longer than the intrinsic time constants of the network elements. Our network is formally not in the low-connectivity limit since the number of neurons $N=800$ is small. Nevertheless, we found that mean-field results can qualitatively predict the rough location of the phase transition of the macroscopic population rate. Moreover, if the input signal is shared between all neurons, a macroscopic readout is sufficient to explain the network performance in an information buffering task. Microscopic properties do, however, play a role if the input is only given to a subset of the network units suggesting that in this case ultra-short term information buffering in connectivity loops is indeed possible.

B. Signal buffering and computing in random nets

Random networks of model neurons have been proposed as powerful computing devices in the context of “liquid” computing [4] or echo state machines [5]. Typically such networks have been endowed with a certain amount of het-

erogeneity, with intrinsic time constants spanning a wide range [4], and potentially a feedback from the readout units back to the network [5]. In this paper we have only considered the simplest case, i.e., a random network of spiking neurons that is completely homogeneous, since all units are characterized by the same parameters (membrane time constant and threshold) and receive the same number of connections. Moreover, we have focused our study on a particularly simple task, i.e., signal buffering. This purification allows us to ask the question of whether random connectivity can yield a significant increase of buffering times beyond the intrinsic time constant of the network elements themselves. We have seen in this paper that even for a delay of one membrane time constant (20 ms), the performance is not very good. In additional simulations we checked that signal reconstruction is reduced to insignificant levels if the delay Δ is increased to 50 ms. Thus the maximum delay Δ for which signal reconstruction is feasible is not significantly different from the intrinsic neuronal time constants. This suggests that, without slow processes such as synaptic plasticity or neuronal adaptation, a purely random network of spiking neurons is not suitable as an information buffer beyond tens of milliseconds.

-
- [1] A. Gupta, Y. Wang, and H. Markram, *Science* **287**, 273 (2000).
- [2] M. Abeles, *Corticonics* (Cambridge University Press, Cambridge, England, 1991); M. Diesmann, M.-O. Gewaltig, and A. Aertsen, *Nature (London)* **402**, 529 (1999).
- [3] W. M. Kistler and C. I. De Zeeuw, *Neural Comput.* **14**, 2597 (2002); V. A. Billock, *Vision Res.* **37**, 949 (1997).
- [4] W. Maass, T. Natschläger, and H. Markram, *Neural Comput.* **14**, 2531 (2002).
- [5] H. Jaeger and H. Haas, *Science* **304**, 78 (2004).
- [6] N. Bertschinger and T. Natschläger, *Neural Comput.* **16**, 1413 (2004).
- [7] C. Langton, *Physica D* **42**, 12 (1990).
- [8] L. Viana and A. Bray, *J. Phys. C* **18** 3037 (1985); I. Kanter and H. Sompolinsky, *Phys. Rev. Lett.* **58**, 164 (1987); M. Mézard and G. Parisi, *Europhys. Lett.* **3**, 1067 (1987); A. Crisanti and H. Sompolinsky, *Phys. Rev. A* **37**, 4865 (1988).
- [9] S. Amari, *IEEE Trans. Syst. Man Cybern.* **2**, 643 (1972).
- [10] B. Derrida, E. Gardner, and A. Zippelius, *Europhys. Lett.* **4**, 167 (1987).
- [11] B. Derrida and Y. Pomeau, *Europhys. Lett.* **1**, 45 (1986).
- [12] N. Brunel and V. Hakim, *Neural Comput.* **11**, 1621 (1999); N. Brunel, *J. Comput. Neurosci.* **8**, 183 (2000).
- [13] J. C. Sprott, *Chaos and Time-Series Analysis* (Oxford University Press, New York, 2003).
- [14] O. L. White, D. D. Lee, and H. Sompolinsky, *Phys. Rev. Lett.* **92**, 148102 (2004).
- [15] NEST Initiative, available at www.nest-initiative.org